*Molecular Vision* 2018; 24:379-393 <http://www.molvis.org/molvis/v24/379>
Received 16 January 2018 | Accepted 16 May 2018 | Published 18 May 2018



# Inflammation and outer blood-retina barrier (BRB) compromise following choroidal murine cytomegalovirus (MCMV) infections

**Jinxian Xu,[1,2] Xinglou Liu,[1,2] Juan Mo,[1] Brendan Marshall,[1] Libby Perry,[1] Zheng Dong,[1,3] Ming Zhang[1,2]**

*[1]Department of Cellular Biology and Anatomy, Medical College of Georgia, Augusta University, Augusta, GA; [2]James and Jean Vision Discovery Institute, Medical College of Georgia, Augusta University, Augusta, GA; [3]Charlie Norwood VA Medical Center, Augusta, GA*

**Purpose:** The purpose of this study was to determine whether the blood–retina barrier is compromised by choroidal murine cytomegalovirus (MCMV) infection, using electron microscopy.
**Methods:** BALB/c mice were immunosuppressed with methylprednisolone and monoclonal antibodies to CD4 and CD8. At several time points post-MCMV intraperitoneal inoculation, the eyes were removed and analyzed with western blotting and immunoelectron microscopy for the presence of MCMV early antigen (EA) and the host protein RIP3. Posterior eyecups from *RIP3*$^{-/-}$ and *RIP3*$^{+/+}$ mice were cultured and inoculated with MCMV. At days 4, 7, and 11 post-infection, cultures were collected and analyzed with plaque assay, immunohistochemical staining, and real-time PCR (RT–PCR).
**Results:** MCMV EA was observed in the nuclei of vascular endothelial cells and pericytes in the choriocapillaris. Disruption of Bruch's membrane was observed, especially at sites adjacent to activated platelets, and a few RPE cells containing some enlarged vesicles were found directly beneath disrupted Bruch's membrane. Some virus particles were also observed in the enlarged vesicles of RPE cells. Levels of the RIP3 protein, which was observed mainly in the RPE cells and the basement membrane of the choriocapillaris, were greatly increased following MCMV infection, while depletion of RIP3 resulted in greatly decreased inflammasome formation, as well as expression of downstream inflammation factors.
**Conclusions:** The results suggest that systemic MCMV spreads to the choroid and replicates in vascular endothelia and pericytes of the choriocapillaris during immunosuppression. Choroidal MCMV infection is associated with in situ inflammation and subsequent disruption of Bruch's membrane and the outer blood–retina barrier.

Retinitis induced by human cytomegalovirus (HCMV) is a serious ocular complication in patients with AIDS [1-7], and before the advent of combination antiretroviral therapy (cART), AIDS-related HCMV retinitis resulted in vision loss and blindness in about 30% of patients with HIV/AIDS [1,2]. Although cART has resulted in a substantial reduction in new cases of AIDS-related HCMV retinitis, it remains a considerable problem in patients with AIDS who do not respond to or who discontinue cART therapy [3-7]. In recent years, numerous reports have tied HCMV retinitis to patients who are HIV-negative [8] while the occurrence of HCMV retinitis in immunosuppressed patients who were undergoing solid-organ or bone marrow transplantation has also been accumulating [9,10]. Other, more recent evidence suggests that HCMV retinitis may even occur after local ocular immunosuppression in patients with no systemic immune dysfunction [11-13]. Chronic HCMV infection has also been shown to be a novel risk factor for wet age-related macular degeneration (AMD) [14,15].

Correspondence to: Ming Zhang, Department of Cellular Biology and Anatomy, Augusta University, R and E Building, Room CB2815, Augusta, GA 30912; Phone: (706) 721-6772, FAX: (706) 721-6120, email: mzhang@augusta.edu

The study of CMV is complicated by the fact that CMVs are species-specific so HCMV cannot be studied in animal models. Therefore, we and others have used murine cytomegalovirus (MCMV) infection of immunosuppressed mice to investigate the mechanism of HCMV-induced retinitis [16-31]. In the course of systemic MCMV infection, virus spreads to the uveal tract of the eye in immunosuppressed mice [29-31], and although viral antigens were not detected in the inner retina [29-31], infection of the choroid was associated with death of terminal deoxynucleotidyl transferase dUTP nick end labeling (TUNEL-positive) photoreceptors in the overlying retina [32]. Nevertheless, it is still unclear whether choroidal MCMV infection induces in situ inflammation and compromise of the blood–retina barrier (BRB). Increasing evidence suggests that RIP kinases 1 and 3 are key decision makers in cell death, inflammation, and innate immunity against pathogens [33-35]. Production of RIP3 is greatly increased post-ocular MCMV infection [20,36]. However, the exact roles of RIP kinases in the defense against ocular infection remain unknown. Therefore, the aim of this study was to determine whether the blood–retina barrier is compromised by choroidal MCMV infection and whether RIP kinases promote inflammation subsequent to choroidal MCMV infection.

## METHODS

*Cells and virus:* MCMV strain K181 was originally provided by Dr. Edward Morcarski (Emory University, Atlanta, GA). Virus isolation and titer determination have been described previously [37]. A fresh aliquot of virus stocks was thawed and diluted to the appropriate concentration for each experiment.

*Antibodies:* Anti-MCMV early antigen (EA) [38] was labeled with fluorescein isothiocyanate (FITC; Sigma-Aldrich, St. Louis, MO) as previously described [39]. Anti-RPE65 was kindly provided by Dr. Michael Redmond (National Eye Institute, National Institutes of Health, Bethesda, MD). Anti-caspase 1, antiphosphorylated NFκB (p-p65), anti-RIP1, anti-RIP3, goat anti-rabbit immunoglobulin G horseradish peroxidase (IgG-HRP), and goat anti-mouse IgG-HRP were purchased from Cell Signaling Technology, Inc. (Danvers, MA). Anti-β-actin was purchased from Sigma-Aldrich (St. Louis, MO). Texas Red–labeled anti-rabbit IgG was obtained from Vector Laboratories (Burlingame, CA).

*Mice:* Six- to eight-week-old female BALB/c mice (Taconic Inc., Germantown, NY) were used in all in vivo experiments. Breeding pairs of *RIP3*$^{-/-}$ mice and control C57BL/6 (*RIP3*$^{+/+}$) were obtained from Genentech Corp (San Francisco, CA). The mice were negative for the mutation of *rd8* as assayed with PCR and were housed in accordance with National Institutes of Health guidelines. The treatment of animals in this study conformed to the ARVO Statement for the Use of Animals in Ophthalmic and Vision Research and was approved by the Institutional Animal Care and Use Committee of Augusta University.

*In vivo experimental plan:* Mice were immunosuppressed by intramuscular injection of methylprednisolone acetate (2 mg per mouse) every 3 days and by intravenous injection of anti-CD4 and anti-CD8 antibodies as previously described [31]. This treatment typically depletes greater than 99% of CD4$^+$ and CD8$^+$ T cells as assayed with flow cytometry of splenocytes [31]. Mice were infected with $5 \times 10^2$ PFU of MCMV K181 or medium as control by intraperitoneal injection 1 day following the administration of antibodies. Mice were euthanized by intramuscular injection of an overdose (5.0 ml/kg) of a mixture of 42.9 mg/ml ketamine, 8.57 mg/ml xylazine at various times post-infection, and the eyes were removed for analysis. In some mice, posterior eyecups (consisting of the RPE, choroid, and sclera) were separated from the neural retinas and further analyzed.

*Posterior eyecup culture:* Three- to four-week-old *RIP3*$^{-/-}$ or *RIP3*$^{+/+}$ mice were euthanized as described above, and the eyes were harvested. Following removal of muscle, connective tissue, and conjunctiva, the anterior portion of the eye was discarded by an incision below the level of the ciliary body. Subsequent to removal of the lens, vitreous, and neural retina, the posterior eyecup (consisting of the sclera, choroid, and a monolayer of the RPE) was attached, with the sclera side facing down, to a sterile membrane filter (Schleicher & Schuell, Dassel, Germany), which was then mounted on a coverslip (Nalge Nunc International, Rochester, NY) with a drop of Matrigel (BD Biosciences, Bedford, MA). The coverslip with the attached eyecup was inserted in a culture tube in 1 ml of culture medium (Dulbecco's modified Eagle's medium [DMEM, GIBCO, Gaithersburg, MD], 10% FBS [fetal bovine serum, Hyclone, Logan, UT]) and incubated in a roller incubator at 37 °C with a rotation rate of 10−15 rpm. Culture medium was changed after 1 day and twice weekly thereafter. Some cultures were inoculated with MCMV ($5 \times 10^5$ PFU/well) for 3 h. At days 4, 7, and 11 post-infection, the cultures were harvested and analyzed with plaque assay, immunofluorescence staining, or real-time PCR as described below.

*Electron microscopy and immunogold staining:* The eyes of the experimental and control mice were immersed in fixative (4% paraformaldehyde, 0.5% glutaraldehyde in 0.1 M cacodylate buffer) overnight at 4 °C. They were then washed in cacodylate buffer, dehydrated in a graded ethanol series, and embedded in resin (Pure Embed 812 mixture; Electron Microscopy Science, Hatfield, PA). Ultrathin sections were stained with uranyl acetate and lead citrate and visualized in a JEM 1230 transmission electron microscope (JEOL USA Inc., Peabody, MA) at 110 kV and imaged with an UltraScan 4000 CCD camera and a First Light Digital Camera Controller (Gatan Inc., Pleasanton, CA). For immunogold staining, additional ultrathin sections were cut and collected on 200 mesh nickel grids. Following etching with 2% $H_2O_2$ in PBS (1X; 120 mM NaCl, 20 mM KCl, 10 mM $NaPO_4$, 5 mM $KPO_4$, pH 7.4) for 20 min, 1 M ammonium chloride in PBS was applied to the grids for 1 h. The grids were then washed, blocked with 0.1% bovine serum albumin (BSA) in PBS for 2–4 h, and floated in primary antibody (anti-MCMV EA or anti-RIP3) overnight at 4 °C. Secondary antibody in the form of either anti-mouse IgG or anti-rabbit IgG Nanogold™ was applied for 2 h at room temperature, and the Nanogold particles were enhanced for 3–8 min with silver enhancement solution (HQ Silver Enhancement kit, Nanoprobes, Yaphank, NY). Following washing with distilled $H_2O$, the grids were stained with 2% uranyl acetate in 70% EtoH and lead citrate, air-dried, and visualized in the electron microscope. For the MCMV EA and RIP3 double antibody labeling experiments, the grids were initially treated with anti-MCMV EA and the appropriate secondary antibody before silver enhancement

with HQ Silver™ for a total of 4 min. The grids were then exposed to anti-RIP3, and following treatment with secondary antibody, the grids were silver enhanced for a further 4 min.

*Immunofluorescence staining:* Posterior eyecup cultures were embedded in optimum cutting temperature (OCT) compound, frozen, and sectioned on a cryostat. The sections were then fixed with 4% paraformaldehyde for 15 min and stained for RPE-65 and/or MCMV EA as described previously [39,40].

*Western blotting analysis:* The eyecups and the neural retinas were separated from the eyes of the MCMV-infected immunosuppressed mice, non-infected immunosuppressed control mice, or healthy mice. Proteins were extracted from frozen tissue samples in each group (each sample contain pool of at least four eyecups or neural retinas), and western blotting was performed as previously described [41-43].

*Real-time PCR:* RNA was extracted from tissues (each sample contained a pool of at least four eyecups) using an Ambion™ PureLink™ RNA Mini Kit (Invitrogen, Carlsbad, CA) according to the manufacturer's instructions. The expression of 84 key genes involved in the function of inflammasomes, including genes encoding inflammasome components (as well as genes involved in downstream signaling and inhibition of inflammasome function), were detected with real-time PCR (RT–PCR; ABI 7900HT, Applied Biosystems, Carlsbad, CA) with the RT$^2$ Profiler™ gene PCR array kit from QIAGEN Inc (Germantown, MD) according to the manufacturer's instructions. Briefly, 400 ng total RNA were mixed with buffer GE to eliminate the DNA at 42 ºC for 5 min followed by adding same volume of reverse-transcription mix. Reverse transcription (RT) were performed at 42 ºC for 15 min and terminated by heating at 95 ºC for 5 min. 10 µl amplification reactions subjected to the thermal cycling. The cycling conditions included 10 min at 95 ºC followed by 40 cycles of 95 ºC for 15 seconds and 60 ºC for 1 min.

*Statistical analysis:* All data were expressed as means ± standard error of the mean (SEM), with n representing the number of mice used in each experimental group. Statistical analyses were used to determine the significance of observed differences between treatment groups in all experiments. Statistical significance was calculated with a *t* test (and a nonparametric test) under column analyses using the GraphPad Prism 7 Analysis tool. A p value of less than 0.05 were considered statistically significant.

## RESULTS

*Electron microscopy reveals in situ inflammation and a compromised outer blood–retinal barrier:* Our previous studies indicated that systemic MCMV disseminated to the choroid of deeply immunosuppressed mice. Although infection of the choroid was associated with the death of photoreceptors in the overlying retina, MCMV antigens were never detected in the RPE layer, and the outer blood–retina barrier appeared intact when visualized with light microscopy [31]. To investigate more closely whether choroidal MCMV infection is associated with in situ inflammation and whether the blood–retina barrier is compromised, we resolved to use electron microscopy. The BALB/c mice were immunosuppressed, and at day 10 post-MCMV intraperitoneal inoculation, eyes were removed from four mice and examined with electron microscopy using routine uranyl acetate staining and immunogold labeling for MCMV EA.

Immunogold-labeled MCMV EA was observed in the nuclei of some vascular endothelial cells and pericytes in the choriocapillaris (Figure 1B), but no gold particles were observed in the RPE layer or in the inner retina. Adherent leukocytes and platelets were also observed in the choriocapillaris, and some appeared activated and were attached to the vessel wall (Figure 1C,D). Bruch's membrane showed areas of disorganization, and some disruption was observed in areas adjacent to activated platelets that were attached to vascular endothelia (Figure 1D). Although the majority of RPE cells in infected mice were indistinguishable from RPE cells in uninfected controls (Figure 1E), a few RPE cells (less than ten in one section) containing some enlarged vesicles were noted directly beneath areas of disruption in Bruch's membrane (Figure 1D,F). Although immunogold-labeled MCMV EA was not observed in the RPE layer, surprisingly, we observed a few virus particles (Figure 2A,B) in the enlarged vesicles of RPE cells located directly beneath disruptions of Bruch's membrane (Figure 2C). Future experiments will determine whether there are any changes in RPE tight junctions in these samples. No infiltrating inflammatory cells were noted in the inner retina.

*Activation of inflammasomes following in vivo choroid MCMV infection:* To determine whether an innate immune response and inflammation are induced via activation of inflammasomes or NFκB following in vivo choroid MCMV infection, caspase 1 and NFκB were analyzed in the eyecups and inner retinas of MCMV-infected and control mice with western blotting. Although similar levels of active NFκB were detected in the eyecups of the MCMV-infected and control mice (Figure 3), the expression of cleaved caspase 1 was increased in the eyecups after MCMV infection (Figure 3), indicating that inflammasomes are activated in the eyecups following systemic MCMV infection of the deeply immunosuppressed mice. Most likely due to immunosuppression, the basal level of cleaved caspase 1 in the

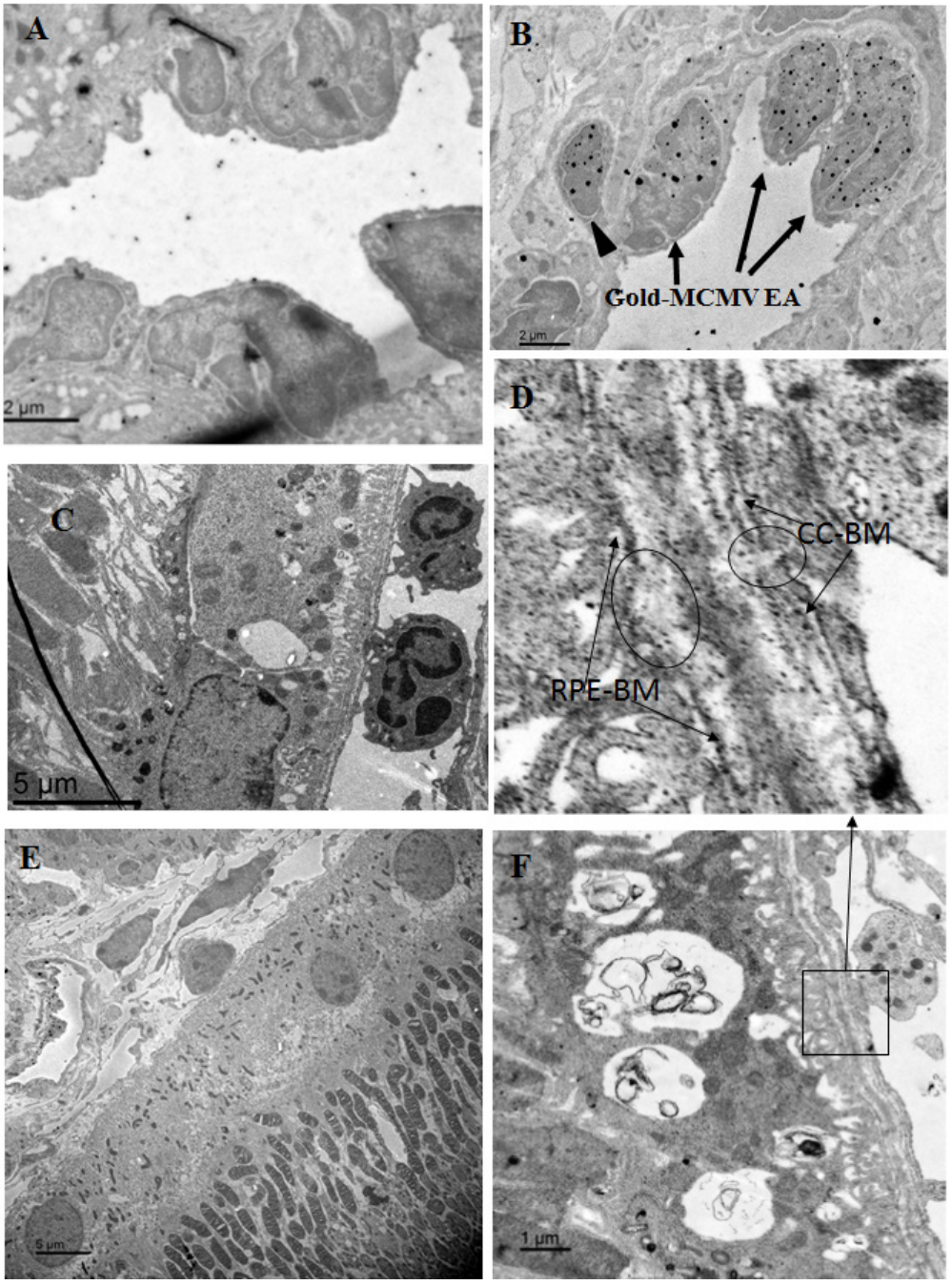


Figure 1. Representative electron microscopic images in eyes from MCMV-injected immunosuppressed mice at day 10 post-infection. **A**: A negative control stained with secondary antibody alone. This shows negligible background staining in the eyes of MCMV infected mice. **B**: Immunogold staining of MCMV EA showing Immunogold-labeled MCMV EA in the nuclei of some vascular endothelial cells (arrows) and pericytes (arrow head) in the choriocapillaris. **C**: Adherent leukocytes in the choriocapillaris. **D**: Disorganization and disruption of Bruch's membrane in areas adjacent to activated platelets which were attached to vascular endothelia. Circles indicate disrupted CC-BM (choriocapillaris basement membrane) and RPE-BM (RPE basement membrane). **E**: The majority of RPE cells in the infected eye were indistinguishable from RPE cells in uninfected controls. **F**: An RPE cell which contained enlarged vesicles was found directly beneath disrupted Bruch's membrane.

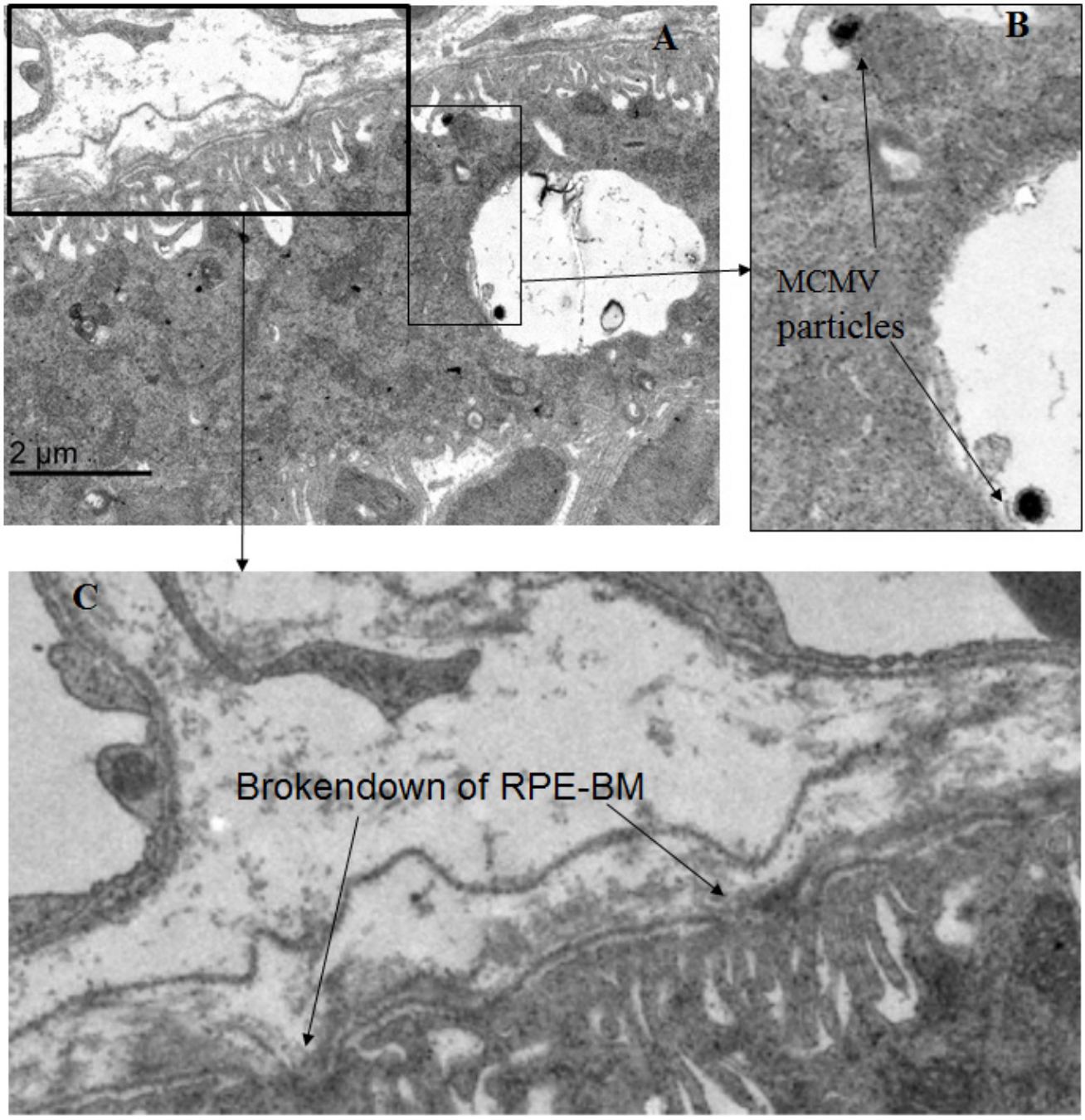


Figure 2. Representative electron microscopic images in eye from a MCMV-infected immunosuppressed mouse at day 10 post-infection. **A**: Virus particles in the enlarged vesicles of RPE cells directly beneath disrupted Bruch's membrane. **B**: Virus particles in enlarged vesicles of RPE cells (arrows). **C**: Disrupted RPE-BM (arrows).

immunosuppressed control group was lower than that in the non-immunosuppressed healthy group (CTR versus Healthy, Figure 3A). There was no difference in the levels of active NFκB and caspase 1 between the inner retinas of the MCMV-infected mice and the control mice.

To investigate which inflammasomes were involved and to identify downstream signaling genes, RNA was extracted from the eyecups of the MCMV-infected and control mice, and the expression of 84 key genes involved in the function of inflammasomes, including genes encoding inflammasome components (as well as genes involved in downstream

signaling and inhibition of inflammasome function), were measured with real-time PCR. The results showed that 47 of the 84 genes showed no statistically significant difference (less than twofold) between the viral infected and control mice, whereas 33 genes were upregulated by twofold or more after viral infection (Table 1). Multiple NOD-like receptors (NLRs), including NLRC5, NLRP3, NLRP4, NLRP6, and the PYHIN family member AIM2, were upregulated in the eyecups of the MCMV-infected mice, indicating that multiple NLRs and AIM2 participate in the formation of inflammasomes. Many inflammatory factors downstream of inflammasome activation, including Nfkbib, Tnf, Ccl12, Ccl5, Ccl7, Cxcl3, Cxcl1, Ifnb1, Il6, and Irf1, were also upregulated in the eyecups of mice systemically infected with MCMV.

*Expression of RIP kinases in the eyecups and retinas following in vivo choroidal MCMV infection:* Increasing evidence suggests that RIP kinases 1 and 3 are key decision makers in cell death, inflammation, and innate immunity against pathogens [33-35]. The preliminary studies also showed that RIP kinases play unique roles in the death of retinal cells, as well as in innate immunity against retinal viral infection following intraocular MCMV infection. To determine whether the production and activation of RIP kinases are affected by choroidal MCMV infection, eyecups and neural retinas were separated from eyes of MCMV-infected and uninfected control mice, and western blotting was performed to detect relative levels of RIP1 and RIP3 proteins. As shown in Figure 4, similar amounts of full-length RIP1 were observed in the eyecups of the MCMV-infected immunosuppressed mice, immunosuppressed control mice, and non-immunosuppressed control mice. In contrast, RIP3 levels were greatly increased in the eyecups of the MCMV-infected immunosuppressed mice, compared to the eyecups of the immunosuppressed or non-immunosuppressed control mice. Although a small amount of cleaved RIP1 was observed in the eyecups of the control mice, more cleaved RIP1 was detected after MCMV infection. Similar amounts of full-length RIP1 and cleaved RIP1 were detected in the retinas of the MCMV-infected immunosuppressed mice and the control mice. RIP3 was almost undetectable in the inner retina of

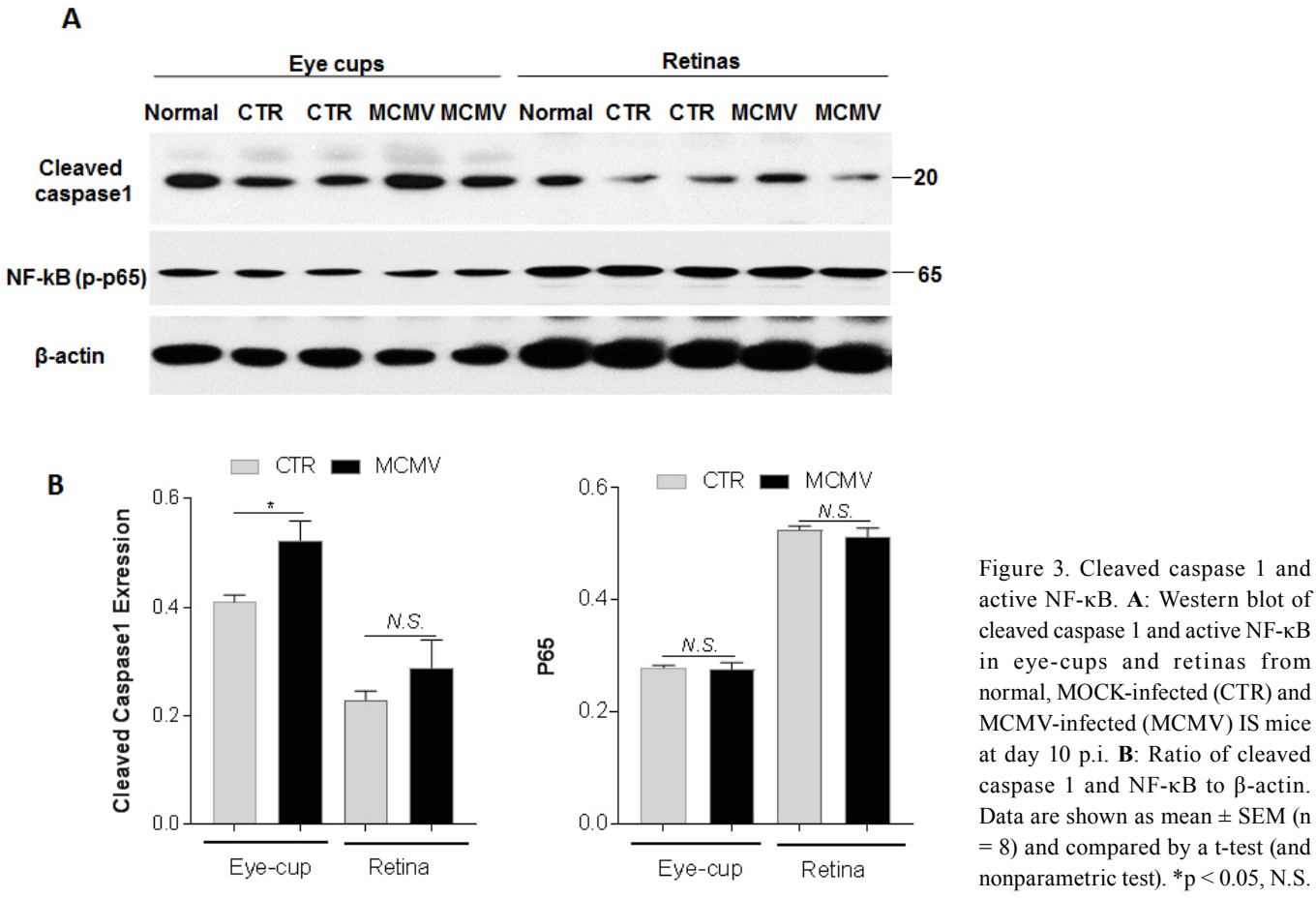


Figure 3. Cleaved caspase 1 and active NF-κB. **A**: Western blot of cleaved caspase 1 and active NF-κB in eye-cups and retinas from normal, MOCK-infected (CTR) and MCMV-infected (MCMV) IS mice at day 10 p.i. **B**: Ratio of cleaved caspase 1 and NF-κB to β-actin. Data are shown as mean ± SEM (n = 8) and compared by a t-test (and nonparametric test). *p < 0.05, N.S. = Not significant.

Table 1. Upregulated genes in eye cup by systemic infection of MCMV (MCMV versus Control).

| Gene Symbol | Gene Description | Fold Regulation |
|---|---|---|
| Aim2 | Absent in melanoma 2 | 3.32 |
| Bcl2l1 | Bcl2-like 1 | 9.35 |
| Birc3 | Baculoviral IAP repeat-containing 3 | 2.71 |
| Casp1 | Caspase 1 | 3.69 |
| Casp12 | Caspase 12 | 2.32 |
| Ccl12 | Chemokine (C-C motif) ligand 12 | 11.99 |
| Ccl5 | Chemokine (C-C motif) ligand 5 | 53.79 |
| Ccl7 | Chemokine (C-C motif) ligand 7 | 52.00 |
| Cd40lg | CD40 ligand | 2.34 |
| Ciita | Class II transactivator | 7.31 |
| Cxcl1 | Chemokine (C-X-C motif) ligand 1 | 53.38 |
| Cxcl3 | Chemokine (C-X-C motif) ligand 3 | 11.04 |
| Ifnb1 | Interferon β1, fibroblast | 19.06 |
| Ifng | Interferon γ | 244.50 |
| Il12a | Interleukin 12A | 34.22 |
| Il1b | Interleukin 1β | 10.22 |
| Il6 | Interleukin 6 | 40.69 |
| Irf1 | Interferon regulatory factor 1 | 5.35 |
| Mefv | Mediterranean fever | 3.92 |
| Myd88 | Myeloid differentiation primary response gene 88 | 2.08 |
| Naip1 | NLR family, apoptosis inhibitory protein 1 | 3.20 |
| Naip5 | NLR family, apoptosis inhibitory protein 5 | 8.42 |
| Nfkbib | Nuclear factor of kappa light polypeptide gene enhancer in B-cells inhibitor, beta | 16.56 |
| Nlrc5 | NLR family, CARD domain containing 5 | 37.03 |
| Nlrp3 | NLR family, CARD domain containing 3 | 2.95 |
| Nlrp4b | NLR family, CARD domain containing 4B | 16.51 |
| Nlrp6 | NLR family, CARD domain containing 6 | 3.43 |
| Nod1 | Nucleotide-binding oligomerization domain containing 1 | 40.81 |
| Nod2 | Nucleotide-binding oligomerization domain containing 2 | 2.64 |
| Tnf | Tumor necrosis factor | 10.21 |
| Tnfsf11 | Tumor necrosis factor (ligand) superfamily, member 11 | 164.90 |
| Tnfsf14 | Tumor necrosis factor (ligand) superfamily, member 14 | 2.70 |
| B2m | Beta-2 microglobulin | 6.55 |

the immunosuppressed and non-immunosuppressed control mice. In contrast, a small amount of RIP3 was observed in the inner retina after systemic infection. As antibody to cleaved RIP3 is not available, we were unable to determine whether RIP3 activation was affected in the eyecup or retina after infection.

Immunogold staining was performed to identify cells in which RIP3 expression was increased following infection. Only sporadic immunogold-RIP3 particles were present in the choroid and RPE cells of the uninfected control mice (Figure 5B), whereas in the choroid and RPE cells of the MCMV-infected mice we observed an approximately 100-fold increase (Figure 5C,D). Some of these RIP3-stained structures inside RPE cells appeared to be mitochondria (Figure 5C, indicated by circles). In addition, many immunogold-RIP3 particles were also observed in the basement membrane of vascular endothelial cells in the choriocapillaris after systemic MCMV infection (Figure 5D). Because

MCMV EA was also observed in some endothelial cells and pericytes in the choriocapillaris, immunogold double staining was performed to colocalize MCMV EA and RIP3 in the choriocapillaris. As shown in Figure 5E, RIP3 (smaller particles indicated by arrows) was observed mainly in the basement membrane of the choriocapillaris between MCMV EA-stained endothelial cells and pericytes. Although a small amount of RIP3 was detected with western blotting in the inner retina after systemic infection, we did not observe any specific immunogold-RIP3-stained cells in the inner retina.

*Depletion of RIP3 decreases the activation of inflammasomes following in vitro MCMV infection of eyecups:* As choroidal MCMV infection is associated with increased production of RIP3 in the choroidal capillaries and RPE cells, we hypothesized that RIP3 might play an important role in the initial innate immune response of resident immune cells in response to choroidal infection. To investigate this possibility and to preclude interference by systemic immune cells or inflammatory cells in the in vivo experiments, an in vitro MCMV-infected eyecup culture model was established to test this hypothesis. In this in vitro model, the posterior eyecup, consisting of the sclera, choroid, and a monolayer of RPE, was attached to a filter which was then mounted on a coverslip with a drop of Matrigel. The coverslip and the filter were inserted into a culture tube in 1 ml of culture medium and incubated at 37 °C at a rotation rate of 15 rpm. The eyecups remained attached to the filters throughout the culture period. Following inoculation with MCMV, replicating virus was recovered from the infected cultures (Figure 6A) while the overall architecture of the cultured eyecups was maintained (Figure 6B). Double staining for MCMV EA and RPE65 showed that RPE-65-positive RPE cells were present at day 11 post-culture MCMV-infected and were infected with MCMV (Figure 6B). In addition, MCMV-infected cells were also observed in the choroid and sclera (Figure 6B). To determine whether the depletion of RIP3 decreased inflammasome formation and the subsequent innate immune response in eyecups following MCMV infection, posterior eyecups were isolated from the eyes of *RIP3*$^{-/-}$ and *RIP3*$^{+/+}$ mice, cultured, and infected with MCMV in vitro. At day 7 post-infection, the infected and uninfected control eyecup cultures were collected and prepared for plaque assay and real-time PCR, to measure the expression of 84 key genes involved in the function of inflammasomes. As shown in Table 2, 23 genes were upregulated in the *RIP3*$^{+/+}$ eyecups by a factor of two or greater at day 7 post-infection. Similar to mRNA expression in the eyecups of the in vivo MCMV-infected mice

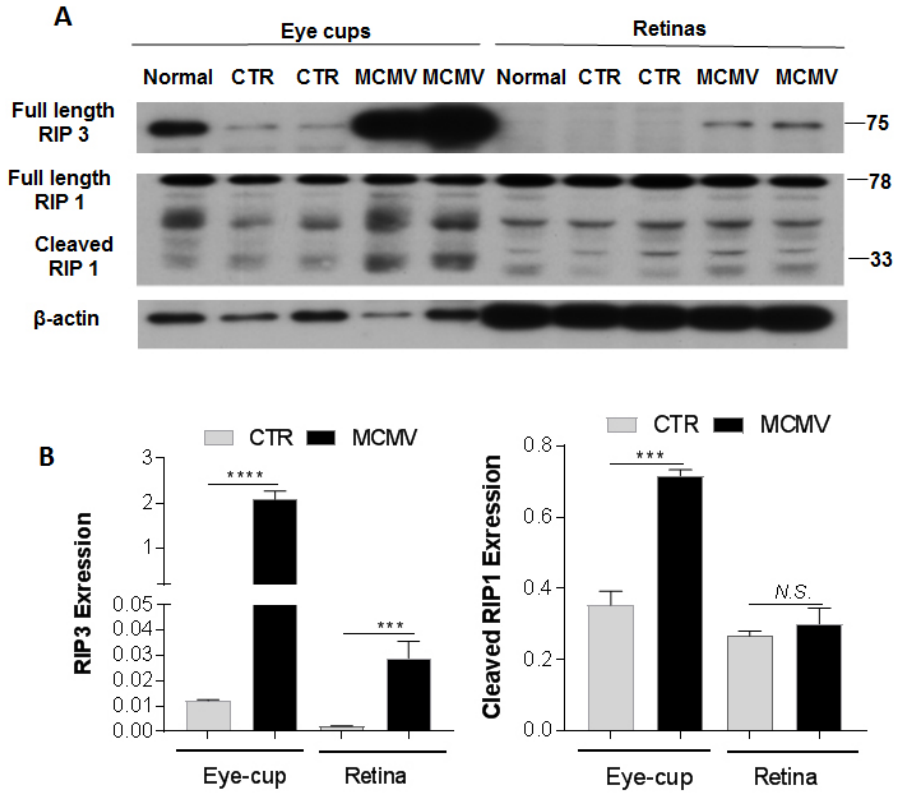


Figure 4. RIP3 and RIP1. **A**: Western blot of RIP3 and RIP1 in eye-cups and retinas from normal, MOCK-infected (CTR) and MCMV-injected IS (MCMV) mice at day 10 p.i. **B**: Ratio of RIP3 and cleaved RIP1 to β-actin. Data are shown as mean ± SEM (n = 8) and compared by a t-test (and nonparametric test). ****p < 0.0001, ***p < 0.001. N.S. = Not significant.

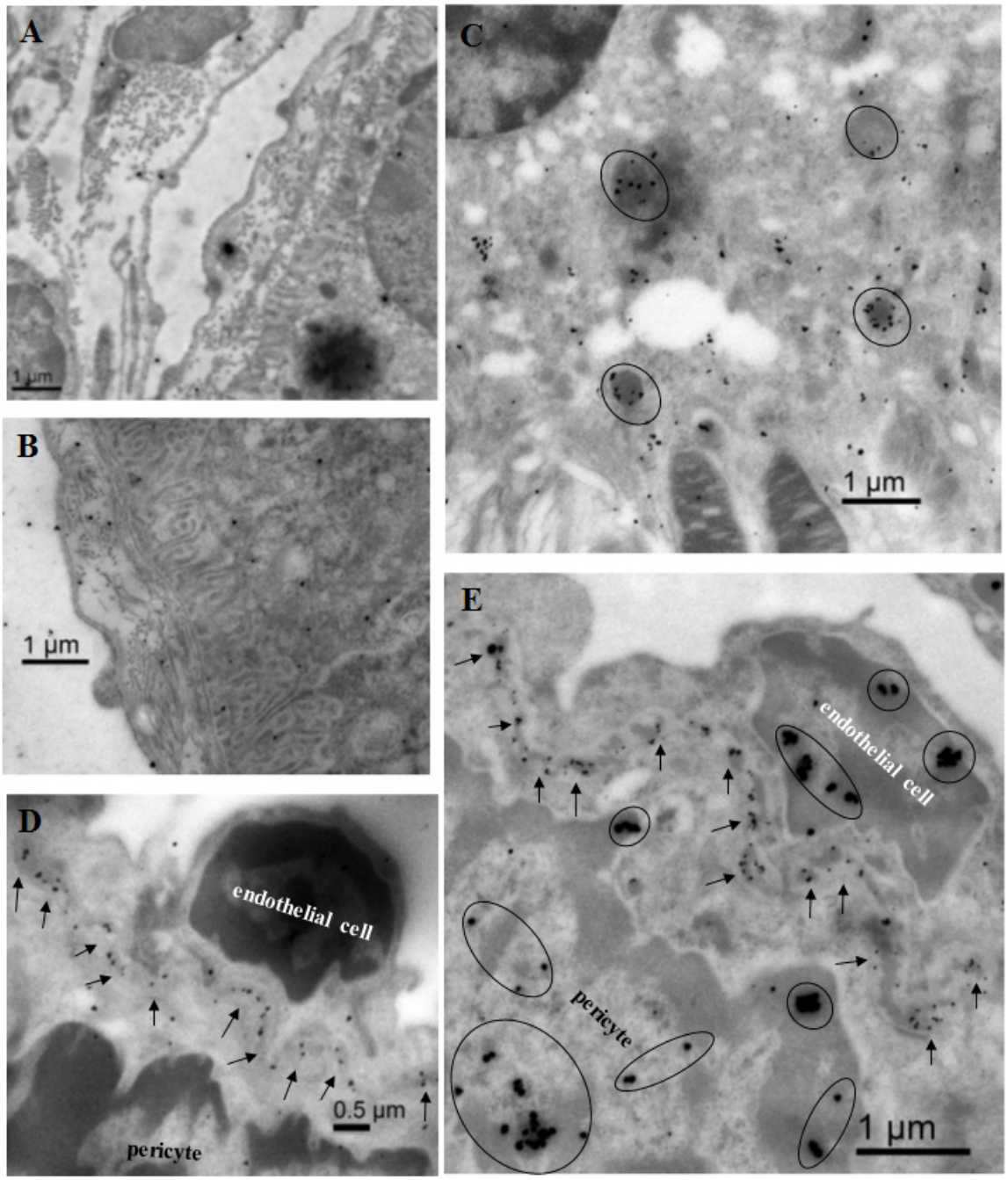


Figure 5. Representative electron microscopic images in eyes from MCMV-infected immunosuppressed mice at day 10 post-infection or from an uninfected control mouse. **A**: A negative control micrograph stained with secondary antibody alone. This shows minimal labeling in the eye of an MCMV infected mouse. **B**: Immunogold staining of RIP3 in the eye of an uninfected control mouse. This shows sparse immunogold-RIP3 particles in the choroid and RPE cells. **C**: Immunogold staining of RIP3 in the eye of an MCMV infected mouse. Many immunogold-RIP3 particles were observed inside the RPE cells, some of these RIP3 stained structures appeared to be mitochondria (circles). **D**: Immunogold staining of RIP3 in the eye of an MCMV infected mouse. Immuogold-RIP3 particles were observed in the basement membrane of vascular endothelial cells in the choriocapillaris. **E**: Double immunogold staining of MCMV EA (Larger particles) and RIP3 (smaller particles) in the eye of an MCMV infected IS mouse. RIP3 (arrows) was observed mainly in the basement membrane of the choriocapillaris between MCMV EA (circled larger particles in the nuclei) stained endothelial cells and pericytes.

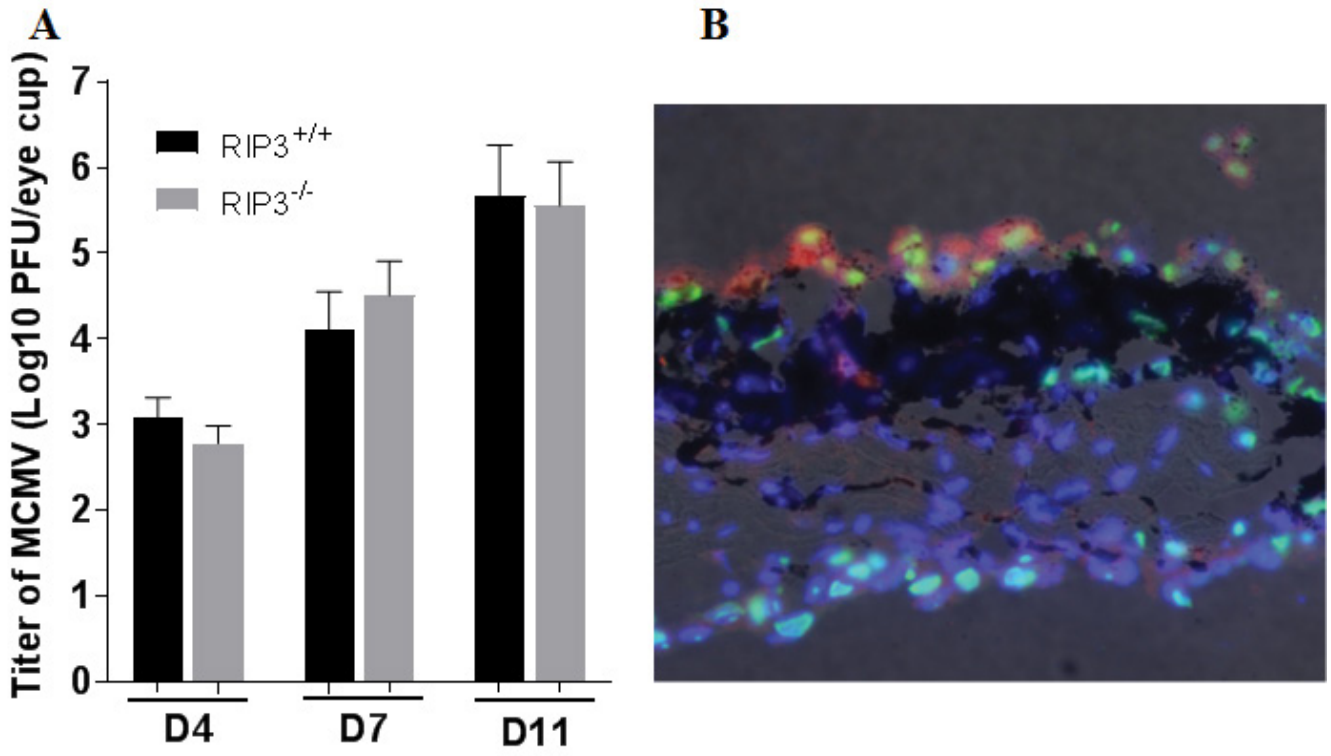


Figure 6. MCMV infected eye-cups. **A**: Titer of MCMV (Log10 ± SEM PFU/ml) in eye-cups isolated from *RIP3*$^{+/+}$ and *RIP3*$^{-/-}$ mice at day 4, 7 and 11 post MCMV inoculation. Data are shown as mean ± SEM (n = 4). **B**: Photomicrograph of MCMV EA (green), RPE65 (red) and DAPI (blue) in an MCMV-infected cultured eye-cup at day 11 pi. RPE-65 positive cells were present and were infected with MCMV. MCMV infected cells were also observed in the choroid and sclera. Original magnification, ×200.

as shown in Table 1, multiple NLRs, including NLRC5, NLRP3, and NLRP6, were upregulated in the *RIP3*$^{+/+}$ eyecup cultures following MCMV infection. Some inflammatory factors downstream of inflammasome activation, including Nfkbia, Tnf, Ccl12, Ccl5, Ccl7, Cxcl1, Cxcl3, Ifnb1, Il6, and Irf1, were also upregulated in the *RIP3*$^{+/+}$ eyecup cultures following MCMV infection. Although similar amounts of MCMV were detected in the *RIP3*$^{-/-}$ and *RIP3*$^{+/+}$ eyecups (Figure 6A), only seven genes were upregulated by a factor of two or greater in *RIP3*$^{-/-}$ eyecups at day 7 post-infection. In addition, the levels of these seven upregulated genes in the MCMV-infected *RIP3*$^{-/-}$ eyecups were lower than in those in the MCMV-infected *RIP3*$^{+/+}$ eyecups (Table 2).

## DISCUSSION

As we previously reported [29-31], the data indicate that virus-infected cells are present in the choroid following systemic inoculation of MCMV into deeply immunosuppressed mice. Although neither virus-infected cells nor infiltrating inflammatory cells were noted in the inner retina, the experiments presented in this study demonstrate for the first time that choroidal MCMV infection is associated with in situ inflammation and disruption of the blood–retina barrier. This barrier, which is present at the base of the RPE (the outer BRB) and the retinal vascular endothelium (the inner BRB), plays an important role in the prevention of virus dissemination to the retina. Compromise of the BRB in HIV-infected individuals has been suggested to promote HCMV infection of the retina leading to retinitis [44-49]. The presence of HIV infection in the retinal vasculature has been reported in patients infected with HIV-infected [46,47] while dual HIV and CMV infection of individual cells in the retinal vasculature has also been noted [48]. Cotton wool spots (CWSs) are the most common fundus finding in HIV infection and occur in almost 50% of patients [44]. It is believed that CWSs are induced either by deposition of immune complexes in the microvasculature or infection of vascular endothelia, resulting in vessel occlusion, and eventually disruption of the BRB [44,45]. However, CWSs are absent in many patients with CMV retinitis [44] while CMV retinitis is not limited to patients with HIV/AIDS [8]. Furthermore, cases of CMV

Table 2. Upregulated genes in cultured eye cup infected with MCMV (MCMV versus Control)

| Genes | *RIP3*$^{+/+}$ | *RIP3*$^{-/-}$ |
|---|---|---|
| Casp1 | 3.38 | 2.06 |
| Ccl12 | 15.71 | 4.09 |
| Ccl5 | 17.59 | 3.50 |
| Ccl7 | 14.78 | 4.55 |
| Cxcl1 | 4.37 | 1.29 |
| Cxcl3 | 3.78 | 1.13 |
| Ifnb1 | 2.63 | 1.13 |
| Ifng | 4.83 | 1.20 |
| IL6 | 13.62 | 4.84 |
| Irf1 | 3.40 | 1.30 |
| Mefv | 4.96 | 1.13 |
| Naip5 | 4.52 | 1.41 |
| NFKbia | 2.30 | 1.13 |
| Nlrc5 | 19.66 | 18.11 |
| Nlrp12 | 2.79 | 0.82 |
| Nlrp3 | 5.58 | 1.55 |
| Nlrp6 | 2.06 | 1.13 |
| ptgs2 | 2.77 | 1.67 |
| Tnf | 2.24 | 1.36 |
| Tnfsf11 | 7.27 | 0.83 |
| Tnfsf4 | 2.06 | 1.00 |
| Txnip | 2.05 | 1.20 |
| B2m | 5.81 | 2.76 |

retinitis in patients who are immunosuppressed for solid-organ or bone marrow transplantation have been accumulating [9,10] while recent evidence suggests that CMV retinitis may even occur in patients who exhibit no systemic immune dysfunction but only local ocular immunosuppression [11-13]. Therefore, there may be multiple routes by which CMV can gain entry into the retina. As the development of CMV retinitis is associated with an elevated viral load and a prolonged period of viremia [10], CMV infection of endothelial cells and pericytes in the choroid capillaries, local inflammation, and disruption of Bruch's membrane in the outer blood–retina barrier should be considered a potential route by which virus enters the retina during periods of viremia.

The present results also suggest that the formation of inflammasomes leading to caspase 1 activation plays an important role in local inflammation following choroidal MCMV infection. Inflammasomes are large, multiprotein complexes formed on a scaffold of cytosolic pattern recognition receptors (PRRs) belonging to the NLR and PYHIN protein families [50-52]. Activation of inflammasomes occurs following the recognition of pathogen-associated molecular patterns (PAMPs) or host-derived damage-associated molecular patterns (DAMPs) by PRRs, resulting in the recruitment and activation of caspase-1 which stimulates the innate immune response through the production of proinflammatory cytokines. The present results indicate that multiple NLRs, including NOD1, NOD2, NLRC5, NLRP3, NLRP4, NLRP6, and the PYHIN family member AIM2, are upregulated in the posterior eyecup following systemic MCMV infection. Among these PRRs, NLRP3, NLRC5, and NLRP6 are also upregulated in eyecup cultures following MCMV infection in vitro, indicating that these three NLRs might play a critical role in the initial innate immune response of resident cells, such as choroidal capillary endothelia and RPE cells against viral infection. Previous studies in other laboratories have also shown that these three NLRs are expressed in endothelia and RPE cells [53-56] and play important roles in regulating inflammation and innate immune responses against viruses and bacteria [51,52,57-62]. NLRP3, for instance, is expressed

in many types of cells, including vascular endothelia [53-55] and RPE cells [56], where it may induce inflammation when activated by DNA or RNA viruses [51,52]. NLRC5 is expressed in most cell types [51] and appears to have context-dependent functions. For instance, NLRC5 has been shown to act as a negative regulator of innate immunity through inhibition of NF-κB and type I IFN-mediated signaling pathways [57,58], whereas NLRC5 can also form inflammasomes with NLRP3 in response to NLRP3 agonists, including bacterial PAMPs and crystals [59]. NLRC5 is activated in human foreskin fibroblasts infected with CMV [59] where NLRC5 plays an important role in the cellular antiviral response by stimulating interferon (IFN) production [60]. NLRP6 is involved in inflammation and host defense against intestinal microorganisms and is highly expressed in intestinal epithelial cells upon challenge with bacteria [61,62].

Several chemokines are expressed downstream of inflammasome activation, including Ccl5, Ccl7, Ccl12, Cxcl1, and Cxcl3, and they are also upregulated in the posterior eyecup following either in vivo systemic or in vitro MCMV infection. These potent chemokines may be involved in the recruitment and activation of leukocytes, thus amplifying the inflammatory response at sites of virus infection. Platelets have been reported to be key regulators of host intravascular immunity and inflammation [63-66], and the present results suggest that some platelets are activated and attached to the walls of damaged capillaries following viral infection. Inflammation induced by activated platelets could contribute to disruption of Bruch's membrane as we often observed membrane compromise at sites near platelet attachment to walls of blood vessels.

RIP kinases 1 and 3 are key decision makers in inflammation and innate immunity against pathogens [33-35] because they participate in activation of the inflammasome/caspase 1 [67-70], and in the case of RIP3 at least, this appears to be independent of its role in programmed necrosis [21,68-70]. Furthermore, RIP kinases have been shown to play diverse tissue-specific roles [71-74], and different disease models in the same organ (liver) have shown various functions for RIP1 and RIP3 [75]. In our experiments, RIP3 production was greatly increased in choroidal capillary walls and RPE cells following systemic MCMV infection, and depletion of RIP3 greatly decreased inflammasome formation, as well as expression of downstream inflammatory factors in MCMV-infected eyecup cultures. Therefore, we conclude that RIP3 plays an important role in the initial innate immune response of in situ residential cells against choroidal MCMV infection via formation and activation of inflammasomes, as this in vitro model of virus infection eliminates potentially confounding effects caused by invasion of systemic immune or inflammatory cells.

## ACKNOWLEDGMENTS

Supported by NIH grant RO1EY026642

## REFERENCES

1. Cohen J. AIDS therapy. New hope against blindness. Science 1995; 268:368-9. [PMID: 7716538].
2. Gallant JE, Moore RD, Richman DD, Keruly J, Chaisson RE. Incidence and natural history of cytomegalovirus disease in patients with advanced human immunodeficiency virus disease treated with zidovudine. The Zidovudine Epidemiology Study Group. J Infect Dis 1992; 166:1223-7. [PMID: 1358986].
3. Palella FJ Jr, Delaney KM, Moorman AC, Loveless MO, Fuhrer J, Satten GA, Aschman DJ, Holmberg SD. Declining morbidity and mortality among patients with advanced human immunodeficiency virus infection. HIV Outpatient Study Investigators. N Engl J Med 1998; 338:853-60. [PMID: 9516219].
4. Holtzer CD, Jacobson MA, Hadley WK, Huang L, Stanley HD, Montanti R, Wong MK, Stansell JD. Decline in the rate of specific opportunistic infections at San Francisco General Hospital, 1994–1997. AIDS 1998; 12:1931-3. [PMID: 9792398].
5. Jacobson MA, Stanley H, Holtzer C, Margolis TP, Cunningham ET. Natural history and outcome of new AIDS-related cytomegalovirus retinitis diagnosed in the era of highly active antiretroviral therapy. Nephrol Dial Transplant 2000; 30:231-3. [PMID: 10619774].
6. Jabs DA, Van Natta ML, Holbrook JT, Kempen JH, Meinert CL, Davis MD. Studies of the Ocular Complications of ARG. Longitudinal study of the ocular complications of AIDS: 1. Ocular diagnoses at enrollment. Ophthalmology 2007; 114:780-6. [PMID: 17258320].
7. Jabs DA. AIDS and ophthalmology, 2008. Arch Ophthalmol 2008; 126:1143-6. [PMID: 18695113].
8. Shapira Y, Mimouni M, Vishnevskia-Dai V. Cytomegalovirus retinitis in HIV-negative patients - associated conditions, clinical presentation, diagnostic methods and treatment strategy. Acta Ophthalmol 2017; [PMID: 29068151].
9. Sanghera NK, Newman TL. Cytomegaloviral retinitis from chronic immunosuppression following solid organ transplant surgery. Clin Exp Optom 2010; 93:261-3. [PMID: 20465550].
10. Jeon S, Lee WK, Lee Y, Lee DG, Lee JW. Risk factors for cytomegalovirus retinitis in patients with cytomegalovirus viremia after hematopoietic stem cell transplantation. Ophthalmology 2012; 119:1892-8. [PMID: 22657564].
11. Vertes D, Snyers B, De Potter P. Cytomegalovirus retinitis after low-dose intravitreous triamcinolone acetonide in an immunocompetent patient: a warning for the widespread

use of intravitreous corticosteroids. Int Ophthalmol 2010; 30:595-7. [PMID: 20931263].

12. Saidel MA, Berreen J, Margolis TP. Cytomegalovirus retinitis after intravitreous triamcinolone in an immunocompetent patient. Am J Ophthalmol 2005; 140:1141-3. [PMID: 16376669].

13. Delyfer MN, Rougier MB, Hubschman JP, Aouizerate F, Korobelnik JF. Cytomegalovirus retinitis following intravitreal injection of triamcinolone: report of two cases. Acta Ophthalmol Scand 2007; 85:681-3. [PMID: 17403022].

14. Miller DM, Espinosa-Heidmann DG, Legra J, Dubovy SR, Suner IJ, Sedmak DD, Dix RD, Cousins SW. The association of prior cytomegalovirus infection with neovascular age-related macular degeneration. Am J Ophthalmol 2004; 138:323-8. [PMID: 15364212].

15. Cousins SW, Espinosa-Heidmann DG, Miller DM, Pereira-Simon S, Hernandez EP, Chien H, Meier-Jewett C, Dix RD. Macrophage activation associated with chronic murine cytomegalovirus infection results in more severe experimental choroidal neovascularization. PLoS Pathog 2012; 8:e1002671-[PMID: 22570607].

16. Bidanset DJ, Beadle JR, Wan WB, Hostetler KY, Kern ER. Oral activity of ether lipid ester prodrugs of cidofovir against experimental human cytomegalovirus infection. J Infect Dis 2004; 190:499-503. [PMID: 15243923].

17. Bidanset DJ, Rybak RJ, Hartline CB, Kern ER. Replication of human cytomegalovirus in severe combined immunodeficient mice implanted with human retinal tissue. J Infect Dis 2001; 184:192-5. [PMID: 11424017].

18. Blalock EL, Chien H, Dix RD. Systemic reduction of interleukin-4 or interleukin-10 fails to reduce the frequency or severity of experimental cytomegalovirus retinitis in mice with retrovirus-induced immunosuppression. Ophthalmol Eye Dis 2012; 4:79-90. [PMID: 23650460].

19. Blalock EL, Chien H, Dix RD. Murine cytomegalovirus downregulates interleukin-17 in mice with retrovirus-induced immunosuppression that are susceptible to experimental cytomegalovirus retinitis. Cytokine 2013; 61:862-75. [PMID: 23415673].

20. Chien H, Dix RD. Evidence for multiple cell death pathways during development of experimental cytomegalovirus retinitis in mice with retrovirus-induced immunosuppression: apoptosis, necroptosis, and pyroptosis. J Virol 2012; 86:10961-78. [PMID: 22837196].

21. Dix RD, Cousins SW. Interleukin-2 immunotherapy of murine cytomegalovirus retinitis during MAIDS correlates with increased intraocular CD8+ T-cell infiltration. Ophthalmic Res 2003; 35:154-9. [PMID: 12711843].

22. Dix RD, Cousins SW. Susceptibility to murine cytomegalovirus retinitis during progression of MAIDS: correlation with intraocular levels of tumor necrosis factor-alpha and interferon-gamma. Curr Eye Res 2004; 29:173-80. [PMID: 15512964].

23. Dix RD, Cousins SW. Cell-mediated cytotoxicity of murine cytomegalovirus-infected target cells allows for release of residual infectious virus. Arch Virol 2005; 150:797-803. [PMID: 15614430].

24. Dix RD, Ekworomadu CO, Hernandez E, Cousins SW. Perforin knockout mice, but not mice with MAIDS, show protection against experimental cytomegalovirus retinitis after adoptive transfer of immune cells with a functional perforin cytotoxic pathway. Arch Virol 2004; 149:2235-44. [PMID: 15503209].

25. Dix RD, Podack ER, Cousins SW. Loss of the perforin cytotoxic pathway predisposes mice to experimental cytomegalovirus retinitis. J Virol 2003; 77:3402-8. [PMID: 12610115].

26. Laycock KA, Fenoglio ED, Hook KK, Pepose JS. An in vivo model of human cytomegalovirus retinal infection. Am J Ophthalmol 1997; 124:181-9. [PMID: 9262541].

27. Laycock KA, Kumano Y, Pepose JS. Reproduction of antiviral effect in an in vivo model of human cytomegalovirus retinal infection. Graefe's archive for clinical and experimental ophthalmology = Albrecht Von Graefes Arch Klin Exp Ophthalmol 1998; 236:527-30. .

28. Prichard MN, Quenelle DC, Bidanset DJ, Komazin G, Chou S, Drach JC, Kern ER. Human cytomegalovirus UL27 is not required for viral replication in human tissue implanted in SCID mice. Virol J 2006; 3:18-[PMID: 16571131].

29. Dix RD. Systemic murine cytomegalovirus infection of mice with retrovirus-induced immunodeficiency results in ocular infection but not retinitis. Ophthalmic Res 1998; 30:295-301. [PMID: 9704333].

30. Gao EK, Yu XH, Lin CP, Zhang H, Kaplan HJ. Intraocular viral replication after systemic murine cytomegalovirus infection requires immunosuppression. Invest Ophthalmol Vis Sci 1995; 36:2322-7. [PMID: 7558728].

31. Zhang M, Xin H, Atherton SS. Murine cytomegalovirus (MCMV) spreads to and replicates in the retina after endotoxin-induced disruption of the blood-retinal barrier of immunosuppressed BALB/c mice. J Neurovirol 2005; 11:365-75. [PMID: 16162479].

32. Bigger JE, Tanigawa M, Zhang M, Atherton SS. Murine cytomegalovirus infection causes apoptosis of uninfected retinal cells. Invest Ophthalmol Vis Sci 2000; 41:2248-54. [PMID: 10892869].

33. Galluzzi L, Kepp O, Krautwald S, Kroemer G, Linkermann A. Molecular mechanisms of regulated necrosis. Semin Cell Dev Biol 2014; 35:24-32.. [PMID: 24582829].

34. Humphries F, Yang S, Wang B, Moynagh PN. RIP kinases: key decision makers in cell death and innate immunity. Cell Death Differ 2015; 22:225-36. [PMID: 25146926].

35. Mocarski ES, Kaiser WJ, Livingston-Rosanoff D, Upton JW, Daley-Bauer LP. True grit: programmed necrosis in antiviral host defense, inflammation, and immunogenicity. J Immunol 2014; 192:2019-26. [PMID: 24563506].

36. Mo J, Marshall B, Covar JA, Zhang NY, Smith SB, Atherton SS, Zhang M. Role of Bax in death of uninfected retinal cells

during murine cytomegalovirus (MCMV) retinitis. Invest Ophthalmol Vis Sci 2014; 55:7137-46. [PMID: 25298417].

37. Atherton SS, Newell CK, Kanter MY, Cousins SW. T cell depletion increases susceptibility to murine cytomegalovirus retinitis. Invest Ophthalmol Vis Sci 1992; 33:3353-60. [PMID: 1330968].

38. Pande H, Campo K, Shanley JD, Creeger ES, Artishevsky A, Gallez-Hawkins G, Zaia JA. Characterization of a 52K protein of murine cytomegalovirus and its immunological cross-reactivity with the DNA-binding protein ICP36 of human cytomegalovirus. J Gen Virol 1991; 72:1421-7. [PMID: 1646282].

39. Zhang M, Xin H, Roon P, Atherton SS. Infection of retinal neurons during murine cytomegalovirus retinitis. Invest Ophthalmol Vis Sci 2005; 46:2047-55. [PMID: 15914622].

40. Zhang M, Xin H, Duan Y, Atherton SS. Ocular reactivation of MCMV after immunosuppression of latently infected BALB/c mice. Invest Ophthalmol Vis Sci 2005; 46:252-8. [PMID: 15623781].

41. Zhou J, Zhang M, Atherton SS. Tumor necrosis factor-alpha-induced apoptosis in murine cytomegalovirus retinitis. Invest Ophthalmol Vis Sci 2007; 48:1691-700. [PMID: 17389501].

42. Zhang M, Marshall B, Atherton SS. Murine cytomegalovirus infection and apoptosis in organotypic retinal cultures. Invest Ophthalmol Vis Sci 2008; 49:295-303. [PMID: 18172106].

43. Zhang M, Covar J, Marshall B, Dong Z, Atherton SS. Lack of TNF-alpha promotes caspase-3-independent apoptosis during murine cytomegalovirus retinitis. Invest Ophthalmol Vis Sci 2011; 52:1800-8. [PMID: 21310911].

44. Skiest DJ. Cytomegalovirus retinitis in the era of highly active antiretroviral therapy (HAART). Am J Med Sci 1999; 317:318-35. [PMID: 10334120].

45. Gonzalez CR, Wiley CA, Arevalo JF, Garcia RF, Kuppermann BD, Berry C, Freeman WR. Polymerase chain reaction detection of cytomegalovirus and human immunodeficiency virus-1 in the retina of patients with acquired immune deficiency syndrome with and without cotton-wool spots. Retina 1996; 16:305-11. [PMID: 8865390].

46. Pomerantz RJ, Kuritzkes DR, de la Monte SM, Rota TR, Baker AS, Albert D, Bor DH, Feldman EL, Schooley RT, Hirsch MS. Infection of the retina by human immunodeficiency virus type I. N Engl J Med 1987; 317:1643-7. [PMID: 3479685].

47. Cantrill HL, Henry K, Melroe NH, Knobloch WH, Ramsay RC, Balfour HH Jr. Treatment of cytomegalovirus retinitis with intravitreal ganciclovir. Long-term results. Ophthalmology 1989; 96:367-74. [PMID: 2540470].

48. Skolnik PR, Pomerantz RJ, de la Monte SM, Lee SF, Hsiung GD, Foos RY, Cowan GM, Kosloff BR, Hirsch MS, Pepose JS. Dual infection of retina with human immunodeficiency virus type 1 and cytomegalovirus. Am J Ophthalmol 1989; 107:361-72. [PMID: 2539019].

49. Kijpittayarit-Arthurs S, Eid AJ, Kremers WK, Pedersen RA, Dierkhising RA, Patel R, Razonable RR. Clinical features and outcomes of delayed-onset primary cytomegalovirus disease in cardiac transplant recipients. J Heart Lung Transplant 2007; 26:1019-24. [PMID: 17919622].

50. Chen IY, Ichinohe T. Response of host inflammasomes to viral infection. Trends Microbiol 2015; 23:55-63. [PMID: 25456015].

51. Jacobs SR, Damania B. NLRs, inflammasomes, and viral infection. J Leukoc Biol 2012; 92:469-77. [PMID: 22581934].

52. Kanneganti TD. Central roles of NLRs and inflammasomes in viral infection. Nat Rev Immunol 2010; 10:688-98. [PMID: 20847744].

53. Bruder-Nascimento T, Ferreira NS, Zanotto CZ, Ramalho F, Pequeno IO, Olivon VC, Neves KB, Alves-Lopes R, Campos E, Silva CA, Fazan R, Carlos D, Mestriner FL, Prado D, Pereira FV, Braga T, Luiz JP, Cau SB, Elias PC, Moreira AC, Camara NO, Zamboni DS, Alves-Filho JC, Tostes RC. NLRP3 Inflammasome Mediates Aldosterone-Induced Vascular Damage. Circulation 2016; 134:1866-80. [PMID: 27803035].

54. Malavige GN, Ogg GS. Pathogenesis of vascular leak in dengue virus infection. Immunology 2017; 151:261-9. [PMID: 28437586].

55. Kinnunen K, Piippo N, Loukovaara S, Hytti M, Kaarniranta K, Kauppinen A. Lysosomal destabilization activates the NLRP3 inflammasome in human umbilical vein endothelial cells (HUVECs). J Cell Commun Signal 2017; 11:275-279. [PMID: 28547650].

56. Marneros AG. NLRP3 inflammasome blockade inhibits VEGF-A-induced age-related macular degeneration. Cell Reports 2013; 4:945-58. [PMID: 24012762].

57. Benko S, Magalhaes JG, Philpott DJ, Girardin SE. NLRC5 limits the activation of inflammatory pathways. J Immunol 2010; 185:1681-91. [PMID: 20610642].

58. Cui J, Zhu L, Xia X, Wang HY, Legras X, Hong J, Ji J, Shen P, Zheng S, Chen ZJ, Wang RF. NLRC5 negatively regulates the NF-kappaB and type I interferon signaling pathways. Cell 2010; 141:483-96. [PMID: 20434986].

59. Davis BK, Roberts RA, Huang MT, Willingham SB, Conti BJ, Brickey WJ, Barker BR, Kwan M, Taxman DJ, Accavitti-Loper MA, Duncan JA, Ting JP. Cutting edge: NLRC5-dependent activation of the inflammasome. J Immunol 2011; 186:1333-7. [PMID: 21191067].

60. Kuenzel S, Till A, Winkler M, Hasler R, Lipinski S, Jung S, Grotzinger J, Fickenscher H, Schreiber S, Rosenstiel P. The nucleotide-binding oligomerization domain-like receptor NLRC5 is involved in IFN-dependent antiviral immune responses. J Immunol 2010; 184:1990-2000. [PMID: 20061403].

61. Wlodarska M, Thaiss CA, Nowarski R, Henao-Mejia J, Zhang JP, Brown EM, Frankel G, Levy M, Katz MN, Philbrick WM, Elinav E, Finlay BB, Flavell RA. NLRP6 inflammasome orchestrates the colonic host-microbial interface by

regulating goblet cell mucus secretion. Cell 2014; 156:1045-59. [PMID: 24581500].

62. Elinav E, Strowig T, Kau AL, Henao-Mejia J, Thaiss CA, Booth CJ, Peaper DR, Bertin J, Eisenbarth SC, Gordon JI, Flavell RA. NLRP6 inflammasome regulates colonic microbial ecology and risk for colitis. Cell 2011; 145:745-57. [PMID: 21565393].

63. Jenne CN, Kubes P. Platelets in inflammation and infection. Platelets 2015; 26:286-92. [PMID: 25806786].

64. Lima-Junior JC, Rodrigues-da-Silva RN, Pereira VA, Storer FL, Perce-da-Silva DS, Fabrino DL, Santos F, Banic DM, Oliveira-Ferreira J. Cells and mediators of inflammation (C-reactive protein, nitric oxide, platelets and neutrophils) in the acute and convalescent phases of uncomplicated Plasmodium vivax and Plasmodium falciparum infection. Mem Inst Oswaldo Cruz 2012; 107:1035-41. [PMID: 23295755].

65. McNicol A, Israels SJ. Beyond hemostasis: the role of platelets in inflammation, malignancy and infection. Cardiovasc Hematol Disord Drug Targets 2008; 8:99-117. [PMID: 18537597].

66. Klinger MH, Jelkmann W. Role of blood platelets in infection and inflammation. J Interferon Cytokine Res 2002; 22:913-22. [PMID: 12396713].

67. Kataoka K, Matsumoto H, Kaneko H, Notomi S, Takeuchi K, Sweigard JH, Atik A, Murakami Y, Connor KM, Terasaki H, Miller JW, Vavvas DG. Macrophage- and RIP3-dependent inflammasome activation exacerbates retinal detachment-induced photoreceptor cell death. Cell Death Dis 2015; 6:e1731-[PMID: 25906154].

68. Philip NH, Dillon CP, Snyder AG, Fitzgerald P, Wynosky-Dolfi MA, Zwack EE, Hu B, Fitzgerald L, Mauldin EA, Copenhaver AM, Shin S, Wei L, Parker M, Zhang J, Oberst A, Green DR, Brodsky IE. Caspase-8 mediates caspase-1 processing and innate immune defense in response to bacterial blockade of NF-kappaB and MAPK signaling. Proc Natl Acad Sci USA 2014; 111:7385-90. [PMID: 24799700].

69. Vince JE, Wong WW, Gentle I, Lawlor KE, Allam R, O'Reilly L, Mason K, Gross O, Ma S, Guarda G, Anderton H, Castillo R, Hacker G, Silke J, Tschopp J. Inhibitor of apoptosis proteins limit RIP3 kinase-dependent interleukin-1 activation. Immunity 2012; 36:215-27. [PMID: 22365665].

70. Weng D, Marty-Roix R, Ganesan S, Proulx MK, Vladimer GI, Kaiser WJ, Mocarski ES, Pouliot K, Chan FK, Kelliher MA, Harris PA, Bertin J, Gough PJ, Shayakhmetov DM, Goguen JD, Fitzgerald KA, Silverman N, Lien E. Caspase-8 and RIP kinases regulate bacteria-induced innate immune responses and cell death. Proc Natl Acad Sci USA 2014; 111:7391-6. [PMID: 24799678].

71. Rickard JA, O'Donnell JA, Evans JM, Lalaoui N, Poh AR, Rogers T, Vince JE, Lawlor KE, Ninnis RL, Anderton H, Hall C, Spall SK, Phesse TJ, Abud HE, Cengia LH, Corbin J, Mifsud S, Di Rago L, Metcalf D, Ernst M, Dewson G, Roberts AW, Alexander WS, Murphy JM, Ekert PG, Masters SL, Vaux DL, Croker BA, Gerlic M, Silke J. RIPK1 regulates RIPK3-MLKL-driven systemic inflammation and emergency hematopoiesis. Cell 2014; 157:1175-88. [PMID: 24813849].

72. Silke J, Rickard JA, Gerlic M. The diverse role of RIP kinases in necroptosis and inflammation. Nat Immunol 2015; 16:689-97. [PMID: 26086143].

73. Kumari S, Redouane Y, Lopez-Mosqueda J, Shiraishi R, Romanowska M, Lutzmayer S, Kuiper J, Martinez C, Dikic I, Pasparakis M, Ikeda F. Sharpin prevents skin inflammation by inhibiting TNFR1-induced keratinocyte apoptosis. eLife 2014; 3:e03422-[PMID: 25443631].

74. Rickard JA, Anderton H, Etemadi N, Nachbur U, Darding M, Peltzer N, Lalaoui N, Lawlor KE, Vanyai H, Hall C, Bankovacki A, Gangoda L, Wong WW, Corbin J, Huang C, Mocarski ES, Murphy JM, Alexander WS, Voss AK, Vaux DL, Kaiser WJ, Walczak H, Silke J. TNFR1-dependent cell death drives inflammation in Sharpin-deficient mice. eLife 2014; 3:e03464-[PMID: 25443632].

75. Deutsch M, Graffeo CS, Rokosh R, Pansari M, Ochi A, Levie EM, Van Heerden E, Tippens DM, Greco S, Barilla R, Tomkotter L, Zambirinis CP, Avanzi N, Gulati R, Pachter HL, Torres-Hernandez A, Eisenthal A, Daley D, Miller G. Divergent effects of RIP1 or RIP3 blockade in murine models of acute liver injury. Cell Death Dis 2015; 6:e1759-[PMID: 25950489].

Articles are provided courtesy of Emory University and the Zhongshan Ophthalmic Center, Sun Yat-sen University, P.R. China. The print version of this article was created on 18 May 2018. This reflects all typographical corrections and errata to the article through that date. Details of any changes may be found in the online version of the article.